Enhancement of urea removal from reclaimed water using thermally modified spent coffee ground biochar activated by adding peroxymonosulfate for ultrapure water production

Xinbo Zhang[a,b,c,1], Yuanying Yang[a,b,1], Huu Hao Ngo[d,a,*], Wenshan Guo[d,a], Tianwei Long[a,b] ,Xiao Wang[e], Jianqing Zhang[e], Fengxia Sun[f]

[a] *Joint Research Centre for Protective Infrastructure Technology and Environmental Green Bioprocess, School of Environmental and Municipal Engineering, Tianjin Chengjian University, Tianjin 300384, China*

[b] *Tianjin Key Laboratory of Aquatic Science and Technology, Tianjin Chengjian University, Jinjing Road 26, Tianjin 300384, China*

[c] *School of Chemistry and Materials Science, University of Science and Technology of China, Hefei, Anhui, 230026, China*

[d] *Centre for Technology in Water and Wastewater, School of Civil and Environmental Engineering, University of Technology Sydney, Sydney, NSW 2007, Australia*

[e] *TG Hilyte Environment Technology (Beijing) Co., LTD., Beijing 100000, China*

[f] *College of Resources and Environment, Shandong Agricultural University, Taian, 271000, China*

[1] Equal contribution

* Correspondence authors: Email: ngohuuhao121@gmail.com (H. H. Ngo)

Abstract

To enhance the degradation of urea in reclaimed water for producing ultrapure water (UPW), thermally modified biochar (TBC) was prepared by secondary pyrolysis using spent coffee biochar with the function as an activator of peroxymonosulfate (PMS). Results showed that 94.4% of urea can be degraded effectively by the TBC-PMS system at the dosage of 0.4 g/L TBC and 2 g/L PMS under neutral and weak acid conditions. Moreover, urea removal mainly depended on the free radical pathway ($SO_4^{\bullet -}$ and $OH^{\bullet}$), especially $OH^{\bullet}$. The inorganic anions of TBC increased via secondary pyrolysis, especially carbonate and phosphate, resulting in higher electrical conductance (EC) value than the original biochar. It was conducive to activating PMS. As well, C-O, -OH worked as an active site in the TBC-PMS system, providing electrons and activating PMS. This work provides a novel strategy for UPW production using TBC-PMS system.

Keywords: Spent coffee ground; Biochar; Ultrapure water; Urea; Persulfate activation

1. Introduction

The modern semiconductor industry is making huge demands for ultrapure water (UPW). For example, it takes about 2200 gallons of water to make an integrated circuit on a 30-centimeter wafer (Zhang et al., 2021). Therefore, what is inevitable is now having to generate reclaimed water to produce UPW, which could supply plentiful raw water and make water recycling more practicable (Wang et al., 2019; Zhang et al., 2021). However, some small molecular organics (e.g., isopropyl alcohol, methanol and urea) can hardly be removed through the traditional UPW system (Choi et al., 2016;

Zhang et al., 2021). So far, the related studies are mainly focused on the overall reduction of conventional organic pollutants in the UPW system, but less attention has been paid to the removal of low concentration urea. Furthermore, Choi et al. (2019) found the TOC in the UPW effluent was positively correlated with the urea concentration in the influent through a long-term monitoring (Choi et al., 2019). Therefore, improving the current UPW system to remove urea in reclaimed water is crucial for ensuring the required effluent quality.

To date, the advanced oxidation processes (AOPs) based on persulfate (PS) are now a research hotspot because of its high efficiency and strong oxidation capacity (Ding et al., 2022; Gao et al., 2022; Yang et al., 2021). For instance, peroxymonosulfate (PMS)-based AOPs have strong oxidation capacity, good stability and convenient transportation while enabling to oxidize a variety of toxic organic pollutants into water and carbon dioxide (Gao et al., 2022; Luo et al., 2020). More importantly, it exhibited better performance in removing urea by being activated through biochar (BC) or activated carbon (Zhang et al., 2022). However, it usually needs to be activated to produce sulfate radicals ($SO_4^{\bullet -}$) with stronger oxidation capacity (Ding et al., 2021). Compared with other activation methods (e.g., transition metal, heating, and ultraviolet (UV)), the BC -PS system can avoid metal leaching and demand no external energy (Wang. et al., 2021; Zhu et al., 2022). Furthermore, BC produced by waste biomass pyrolysis has plenty of practical advantages such as simple preparation, low price and is environmentally friendly (Zhong et al., 2021; Zhu et al., 2022). It is proposed to introduce a BC-PS system into the UPW system as an auxiliary method to remove urea

from reclaimed water in the pretreatment stage.

It has been documented that the catalytic performance of unmodified BC was relatively poor and easy to inactivate, making it challenging to produce a good outcome (Dai et al., 2020; Kim and Ko, 2020; Zhong et al., 2021). Several subsequent modifications are indispensable to improving the catalytic performance of BC, such as doping heteroatoms and loading transition metal (Zhong et al., 2021). However, these modification methods may induce only a low product yield at high production costs, and in the meantime metal leaching will cause secondary pollution (Dai et al., 2020). Therefore, a secondary pyrolysis method was proposed to modify BC in this research. Specifically, the original BC was prepared from spent coffee grounds.

Coffee is one of the most favorable beverages, which consumed worldwide around 166.63 million 60 kilogram bags in 2020/21 (Ridder, 2022). At present, most of them are treated by open-air incineration and landfill, which can cause various environmental problems and waste of resources (Zhang et al., 2020). Therefore, it was proposed to use spent coffee grounds as raw materials to prepare biochar. However, the structure of BC is more complex than commercial granular activated carbon, which may cause the unstable activation effect and more complicated catalytic mechanism (Gao et al., 2022; Lee et al., 2020a; Zhang et al., 2022). Furthermore, based on the previous study, it was known that the removal rate of urea by such BC still needed to be improved and a large amount of oxidant was required, leading to a high removal cost (Zhang et al., 2022). As a result, it is necessary to prepare modified biochar to enhance the catalytic performance. It was found that the oxygen functional group, carbon structure, specific surface area

and pore volume of BC affected the PMS activation (Zhang et al., 2022). Some changes of these structure and physicochemical properties of BCs were caused by secondary pyrolysis, which probably act synergistically to produce free radicals and promote the catalytic reaction (Kim and Ko, 2020; Pan et al., 2021). Compared with loading metal or doping heteroatoms, this method has the benefits of minimal energy consumption, low cost, more environmental protection and more conducive to the actual UPW production.

This work focused on making valuable use of spent coffee grounds and realizing urea removal in reclaimed water, which provided a new pathway for UPW production. The specific objectives of this study are to: (1) prepare modified BC by the secondary pyrolysis method and characterize the physicochemical properties; (2) evaluate the catalytic performance of modified BC; (3) investigate the effects of various parameters on urea degradation, including PMS and catalyst dosages, pH value and coexisting anions; and (4) clarify the activation mechanism preliminarily and assess the role of the modified BC in this catalytic system.

2. Materials and methods

2.1 Materials

Urea (CH_4N_2O, analytical grade), Peroxymonosulfate (PMS, $2KHSO_5 \cdot KHSO_4 \cdot K_2SO_4$) and 5,5-dimethyl-1-pyrroline N-oxide (DMPO) were obtained from Shanghai Macklin Biochemical Share Co., Ltd. (Shanghai, China). All reagents or chemicals were used directly without further purification. UPW (resistivity ≈18.2 mΩ·cm) produced in

the laboratory was employed to prepare aqueous urea solutions in the experiments.

The preparation method of thermal modified BC was as follows. Firstly, the original BC was prepared according to the methods in the previous study (Zhang et al., 2022). Briefly, the waste coffee grounds collected were calcined in a muffle furnace at 900 ℃ and the pyrolysis heating rate was 5 ℃/minute. The obtained black material was original BC. Subsequently, the original BC was placed in the ceramic crucible and put into the muffle furnace again at the calcination temperature of 550 ℃ and the pyrolysis heating rate of 2 ℃/min (Gao et al., 2018; Kim and Ko, 2020). It was then kept at the temperature for 4 hours. After natural cooling, the gray solids obtained were the thermal modified BC, which was recorded as TBC.

2.2 Characterizations

The valence state of elements was observed by X-ray photoelectron spectrometry (XPS). The specific surface area and porosity of catalysts were determined by the Brunauer-Emmett-Teller (BET) method. The surface functional groups of catalysts were analyzed through Fourier transform infrared (FTIR). In addition, the detection method of pH value and electrical conductance (EC) was as follow (Hu et al., 2020). 1 g catalysts and 20 mL UPW were blended and then oscillated at 150 rpm and 25 ℃ for 24 hours. Afterwards, the suspension was detected.

2.3 Experimental procedure

Experimental procedure was divided into catalytic experiment and adsorption experiment. All experiments were done in triplicate. The specific experimental steps are shown as follow.

2.3.1 Catalytic experiments

All catalytic experiments were carried out in a 500 mL conical flask. The initial pH was nearly 7 without any adjustment. Firstly, BC or TBC was added to the urea solution (1 mg/L), and then added the PMS to initiate the catalytic reaction. In order to guarantee sufficient reaction, the conical flask was placed in the shaker and reacted for 5 hours (180 rpm, 25 °C). In addition, quenching experiments were accomplished to further investigate the radicals' role. MeOH and TBA were selected to quench $SO_4^{\bullet -}$ and $OH^{\bullet}$, respectively (Ren et al., 2019). PMS concentration was chosen as 0.8 g/L, 1 g/L, 2 g/L, 4 g/L and 6 g/L to explore the effects of PMS dosage with the constant urea concentration (1 mg/L) and catalyst dosage (0.2 g/L).

2.3.2 Adsorption experiments

Similar to catalytic reaction, adsorption experiments were also prepared in a 500 mL conical flask. The initial pH of the reaction solution was not adjusted and remained in the vicinity of 7. Firstly, 400 mL urea solution with a concentration of 1 mg/L was put into the conical flask. Subsequently, BC or TBC was added into the reaction solution. And then the conical flask was placed in the shaker and reacted for 5 hours (180 rpm, 25 °C).

2.4 Analytical methods

UV-Vis spectrophotometer (Island Ferry, UV-2600) was used to determine the urea concentration through the 2,3-Butanedione monoxime method. The specific steps were as follows: 10 mL water sample, 15 mL UPW, 1 mL 2,3-Butanedione monoxime solution and 2.0 mL antipyrine solution were added in sequence and then mixed.

Afterwards, the mixture was bathed in water at 90℃ for 50 minutes. Finally, the cooled mixture samples were tested at 460 nm. The electron paramagnetic resonance (EPR) spectra were utilized to examine the reactive radicals generated. Specifically, 1 mL 100 mmol DMPO was added into 2.0 mL centrifuge tube containing reaction solution. After shaking, the EPR experiment was started at room temperature. The instrument settings in the EPR test were the default settings.

To statistically evaluate the effect of PMS dosage, catalyst dosage, initial pH and co-existing ions on urea, a one-way analysis of variance (ANOVA) was conducted using EXCEL software (Microsoft Office, USA).

3. Results and discussion

3.1 Characteristics of carbon-based materials

As can be seen from Table 1, the pH value of TBC was much higher than BC. It was due to the secondary pyrolysis increasing the basic groups of BC and reducing the acidic groups (Kim and Ko, 2020). Other researches also confirmed that the pyrolysis process retained most of the inorganic components in the BC, bringing about an increase in the base cations and carbonates (Hu et al., 2020). As a result, TBC exhibited a higher pH value than BC. In addition, the EC value of TBC was dramatically enhanced, indicating that the salinity in TBC suspensions may be higher, which may lead to a stronger conductivity; it was conducive to accelerating mass transfer and promoting catalytic reaction. Therefore, it can be speculated that secondary pyrolysis led to a large loss of volatile substances in BC and increased the inorganic anions and salinity.

Table 1 Physicochemical properties of BC and TBC

Apparently, the specific surface area of TBC shrunk after secondary pyrolysis, while the average pore diameter increased (Table 1). Judging by the nitrogen adsorption/desorption isotherms of BC and TBC (Fig. S1), BC clearly conformed to type I isotherms and no obvious hysteresis loops can be observed. The hysteresis loops owing to capillary condensation in mesopores, which leads to the non-overlap of the nitrogen adsorption/desorption isotherms. It can be inferred from results that BC was mainly composed of micropores (Kim and Ko, 2020). In contrast, TBC conformed to type II isotherms, which was often encountered when the adsorbent pore size was greater than 20 nm. It was consistent with the data about pore diameter in Table 1, indicating that TBC featured only limited micropores. Furthermore, it can be seen from the pore distribution that the micropores of BC appeared to be more than that of TBC, which may also cause a reduction in TBC's specific surface area and pore volume (Kim and Ko, 2020).

With respect to FTIR spectra, many new peaks can be observed in TBC. Besides, the vibration intensity of some peaks was significantly enhanced compared with BC (Fig. S2). Specifically, the peak at around 3441 cm^{-1} and 1635 cm^{-1} corresponded to the stretching vibration of -OH and aromatic C=O, respectively (Li et al., 2020a; Zhang et al., 2022). Obviously, the content of -OH and aromatic C=O increased after secondary pyrolysis. The double peak of TBC in the 1408-1472 cm^{-1} range belonged to the antisymmetric stretching of carbonate, while the weak peak near 864 cm^{-1} represented the out of plane bending of carbonate. It can be inferred that BC modified by secondary

pyrolysis method contained more carbonate groups. The bands around 572 cm^{-1} and 1059 cm^{-1} belonged to the symmetric and asymmetric stretching vibration of P-O-P bond, respectively. In addition, the peak intensity at 1059 cm^{-1} was obviously strong. It meant that TBC contained plenty of pyrophosphate and metaphosphate groups (El-Lateef et al., 2019).

3.2 Evaluation of urea removal

3.2.1 Adsorption of urea by thermally modified biochar

The adsorption capacity of BC and TBC on urea was exhibited in Fig. S3. BC can adsorb about 10% urea at the dosage of 0.2 g/L. However, the adsorption ability of TBC on urea worsened, presumably caused by the small specific surface area and low micropore rate of TBC. In fact, large pore diameter discouraged adsorbing small polar molecular organics with high water solubility such as urea (Zhang et al., 2021). Clearly, the adsorption capacity of BC and TBC on urea was not ideal (Fig. S3). This was mainly caused by two factors. Firstly, BC and TBC are hydrophobic, resulting in their low affinity for hydrophilic urea (Clurman et al., 2020). Secondly, small concentrations of urea increased the mass transfer resistance between urea and adsorbate, hindering the adsorption reaction (Liu et al., 2013). In summary, it was found that BC or TBC alone was not effective in removing small concentrations of urea. For this reason, the effect of removing urea by the catalytic system with PMS was further investigated.

3.2.2 Removal of urea by the thermally modified biochar-peroxymonosulfate system

To determine the catalytic performance of TBC, the activation properties of BC and TBC for PMS were compared (Fig. 1). After coupling with PMS, the degradation rates of urea rose extensively and reached 70% and 91.4% corresponding to BC-PMS and TBC-PMS, respectively. Compared with BC-PMS, the TBC-PMS system removed urea better, indicating that secondary pyrolysis significantly improved catalytic performance. Overall, the better catalytic capacity of TBC was caused by two factors as follows. On one hand, secondary pyrolysis raised the content of inorganic anions, which contributed to the formation of radicals and promoted PMS activation (Pan et al., 2021; Zhu et al., 2020). On the other hand, the EC value of BC was enhanced via secondary pyrolysis. A higher EC value was beneficial to the mass transfer, electron transfer and free radical production in the catalytic reaction and thereby promoted urea degradation.

Fig. 1. Urea removal effect in the catalytic system (BC concentration: 0.2 g/L, TBC concentration: 0.2 g/L, urea concentration: 1 mg/L; C_0 and C_t represent the urea concentration (mg/L) in the solution before and after the degradation reaction, respectively. (Having the same letter: no significant difference, having different letters: significant difference. Results obtained from ANOVA (α = 0.05))

In addition, BC can barely activate PMS at low PMS concentration (<4g/L) (Fig. 1), resulting in poor urea degradation. Specifically, at the PMS concentration of 0.8 g/L, BC-PMS system only achieved 7% urea removal. As can be seen from Fig. 1, the removal rate increased with the rise of PMS dosage, and reached as much as 70% when

6 g/L PMS was added. It can be deduced that higher PMS dosage was favorable to producing more radicals. Further, the effect of removing urea by TBC-PMS system was greatly improved compared with BC-PMS system, and the maximum removal rate can reach 91.4% at the PMS dosage of 2 g/L. However, the urea removal efficiency dropped as PMS concentration continued to go up more than 2 g/L. It was possible that the excessive PMS inhibited urea degradation. Similar results were found elsewhere (Lee et al., 2020b; Wei et al., 2016). It may be caused by the sulfate anion produced by excessive PMS, which might deter the generation of free radicals (see Eq. (1) (Lee et al., 2020b)).

$$2SO_4^{\bullet -} + HSO_5^- \rightarrow 2SO_4^{2-} + HSO_5^{\bullet -} \quad (1)$$

Overall, the PMS dosage was an essential factor affecting the urea removal efficiency. In the BC-PMS system, a larger PMS dosage was more conducive to removing urea. It was speculated that an inflection point appeared when the PMS dosage was expanded. However, excessive PMS extremely enlarged the treatment cost. In addition, sulfate ions will be inevitably produced in large quantities and increase the pressure of subsequent treatment. Zhang et al. (2022) explored the urea removal effect of the BC (obtained from 900 ℃ pyrolysis) -PMS system, and the results showed that the best removal rate was 70% at the PMS dosage of 6 g/L. In addition, the removal rate of BC (obtained from 600 ℃ pyrolysis) -PMS system could only reach 57% (Zhang et al., 2022). Obviously, the substitution of TBC had greatly improved this drawback, which can activate PMS effectively and achieve a better removal outcome with less

PMS. Meanwhile, it was cheap and easy to prepare TBC, so it was expected to be introduced into the UPW system as a new carbon-based material for activating PMS.

3.3 Effect of factors on urea degradation

3.3.1 Effect of thermally modified biochar dosage

Judged from the effect of TBC dosage on urea degradation (Fig. 2 (a)), the urea removal efficiency raised from 40% to 94.4% when TBC dosage increased from 0.05 g/L to 0.4 g/L. The catalyst dosage also affected the catalytic reaction in that a higher catalyst dosage can contribute more active sites to activate PMS (He et al., 2019). Nevertheless, as TBC dosage rose to 0.8 g/L, the removal efficiency diminished to 64%. Similar conclusions have been documented by Luo et al. (2020). As reported, it was due to the competition between excessive TBC and radicals (Luo et al., 2020).

Fig. 2. The effect of TBC dosage (a), pH (b) and co-existing anions (c) in the TBC/PMS system (PMS concentration: 2 g/L, urea concentration: 1 mg/L; C_0 and C_t represent the urea concentration (mg/L) in the solution before and after the degradation reaction, respectively. (Having the same letter: no significant difference, having different letters: significant difference. Results obtained from ANOVA (α = 0.05))

3.3.2 Effect of initial pH

PMS and free radicals existed in different ways at different pH, hence the initial solution pH can significantly affect the catalytic performance (Abdul et al., 2021). As can be seen from Fig. 2 (b), the urea degradation rates remained between 90 %-91 % when the initial pH levels were in the range of 3.0-7.0. The initial pH value had little effect on urea degradation between 3.0 and 7.0. However, as the initial pH levels were up to 8.0, 9.0 and 10.0, the removal efficiency declined to 76%, 74% and 68%,

respectively. The experiment results revealed that the TBC-PMS system exhibited the great urea removal performance under a neutral and weak acid condition (3.0 ~ 7.0). This could be explained as follows. A high initial pH value reduced the proportion of HSO_5^- in the reaction solution. When the pH value was higher than 9.4, SO_5^{2-} was dominant. Compared with SO_5^{2-} (SO_5^{2-}/ SO_4^{2-} = 1.22 V), HSO_5^- (HSO_5^-/ SO_4^{2-} = 1.75 V) was much more oxidative and significantly less difficult to react (Feng et al., 2017).

Furthermore, the pH value of urea solution (1 mg/L) without adjustment was about 7, indicating that the removal effect of the TBC-PMS system can be well adapted to the actual situation. On the other hand, in the actual UPW system, it is necessary to reduce the PMS dosage and avoid excessive sulfate ions from aggravating the burden of desalination processes such as reverse osmosis. Clearly, the TBC-PMS system greatly reduced the PMS dosage compared with BC-PMS.

3.3.3 Effect of co-existing anions

Generally, anions such as Cl^-, HCO_3^-, SO_4^{2-}, and NO_3^- can react with active oxidizing substances and affect the performance of catalytic reaction (Ghauch et al., 2017; Meng et al., 2020). Considering the practical application, the effects of common anions (Cl^-, HCO_3^-, SO_4^{2-} and NO_3^-) were investigated. As shown in Fig. 2 (c), the urea removal efficiency of 91.4% was obtained in the absence of co-existing anions. However, in the presence of 10 mM anions, the urea degradation efficiencies dropped significantly to 55%, 68% and 74%, corresponding to HCO_3^-, SO_4^{2-} and NO_3^-, respectively. The inhibition of these anions on urea removal followed the sequential

order of HCO_3^- > SO_4^{2-} > NO_3^-. It can be explained that these anions scavenged free radicals or reacted with them and formed weaker types of radicals (Eqs. (2)-(4)) (Ghauch et al., 2017; Wang et al., 2017). Among these anions, NO_3^- had only the slightest inhibition on urea degradation, because it reacted slowest with $SO_4^{\bullet-}$ (5.0×10^4 $M^{-1}s^{-1}$ (Wang et al., 2017)). Similarly, the addition of SO_4^{2-} also diminished urea removal to a certain extent, due to the reaction between $SO_4^{\bullet-}$ and SO_4^{2-} (Abdul et al., 2021). Generally, HCO_3^- was regarded as an efficient $SO_4^{\bullet-}$ and $OH^{\bullet}$ scavenger, because it quenched $SO_4^{\bullet-}$ (1.6×10^6 $M^{-1}s^{-1}$) and $OH^{\bullet}$ (8.5×10^6 $M^{-1}s^{-1}$) immediately to produce less reactive carbonate radicals (Eqs. (2) - (3)) (Golshan et al., 2018). Therefore, HCO_3^- had a most clear-cut inhibitory effect on the performance of TBC-PMS system.

Different from the above anions, when 10 mM Cl^- existed in the solution, the urea degradation rate increased to 94% (Fig. 2 (c)), which agreed well with the outcomes exhibited in the previous studies (Tan et al., 2017). It was speculated that $SO_4^{\bullet-}$ can react with Cl^- to form $Cl^{\bullet}$, inducing the enhancement of oxidative power of the reaction medium (Eq. (5) (Ghauch et al., 2017)). Furthermore, Cl^- can react with PMS to produce active chlorine species such as HOCl and Cl_2 (Eqs. (6)- (7)), which can also take part in the degradation process (Nie et al., 2019). Based on the above results, it can be deduced that different anions wielded various degrees of influence on the performance of TBC-PMS. The effect of co-existing anions would largely depend on their molar ratios to PMS (Wang et al., 2020). Therefore, the effect of different concentrations of co-existing anions and the overall effect of two or more of these

anions should also be further explored. Also, the effect of other co-existing cations/organics (e.g., Fe and alcohols) that would compete for bonding with TBC or PMS should also be tested.

$$HCO_3^- + SO_4^{\bullet -} \rightarrow HCO_3^{\bullet} + SO_4^{2-} \quad (2)$$

$$HCO_3^- + OH^{\bullet} \rightarrow CO_3^{\bullet -} + H_2O \quad (3)$$

$$NO_3^- + SO_4^{\bullet -} \rightarrow NO_3^{\bullet} + SO_4^{2-} \quad (4)$$

$$Cl^- + SO_4^{\bullet -} \rightarrow SO_4^{\bullet -} + Cl^{\bullet} \quad (5)$$

$$Cl^- + HSO_5^- \rightarrow SO_4^{2-} + HOCl \quad (6)$$

$$2Cl^- + H^+ + HSO_5^- \rightarrow SO_4^{2-} + Cl_2 + H_2O \quad (7)$$

3.4 Urea degradation mechanism using the thermally modified biochar-peroxymonosulfate system

3.4.1 Identification of active species

Free radicals are common species in PMS activation systems (Wan et al., 2019). In general, the contribution of free radicals to urea removal was investigated via quenching experiments. When a quencher is added, the degree of inhibition can reveal the role of corresponding free radical in the system (Li et al., 2020b; Wan et al., 2019). Specifically, the best urea degradation rate was 91.4% in the absence of quenchers. However, the addition of scavengers sharply reduced the urea degradation rate (see Fig. 3 (a)). When TBA and MeOH were added separately, the urea degradation rate fell to 35.6% and 24.3%, respectively. Results showed that both $OH^{\bullet}$ and $SO_4^{\bullet -}$ contributed to the urea degradation of 67.1% in TBC-PMS system, and $OH^{\bullet}$ played a most significant role (55.8% urea removal) (Fig. 3 (b)).Therefore, it can be concluded that the radical pathway dominated the urea removal in TBC-PMS system. Of note, 91.4 % of urea degradation was reached in the TBC-PMS system, while 26.4 % of urea was removed in

the presence of only PMS, which can be inferred that urea can be degraded through the direct reaction between PMS and urea (Eq. (8))(Choi and Chung, 2019).

Fig. 3. (a) Effect of quenching agent on urea removal in TBC-PMS and PMS-only systems (Having the same letter indicates no significant difference, different letter indicates significant difference. Results obtained from ANOVA (α = 0.05).); (b) Contribution of each radical to urea removal.

The free radical pathway in TBC-PMS catalytic system was further proved by quenching experiments and made a contribution of about 65%. Specifically, combined with the results of TBA quenching experiment, it can be deduced that the contribution of $SO_4^{\bullet -}$ and $OH^{\bullet}$ was about 11.3% and 53.7%, respectively. Obviously, $OH^{\bullet}$ was the main contributor in TBC-PMS system, which was produced via the reaction of $SO4^{\bullet -}$ with water (see Eq. (9)) (Ghauch et al., 2017). According to previous studies, free radicals can oxidize urea into nitrate, carbon dioxide and water (Choi et al., 2019; Kim et al., 2019). Compared with adding PMS alone, the TBC-PMS system greatly enhanced urea removal capacity, indicating that TBC did play a vital role of catalyst in the system:

$$CO(NH_2)_2 + 7H_2O + 8Na_2S_2O_8 \rightarrow CO_2 + 2NO^{3-} + 16Na^+ + 16\ SO_4^{2-} + 18H^+ \quad (8)$$

$$SO_4^{\bullet -} + H_2O \rightarrow OH^{\bullet} + HSO_4^- \quad (9)$$

Further, the free radicals in the TBC-PMS system were confirmed by EPR (DMPO as radical trapping agent) (see Supplementary Materials). The representative signals (1:2:2:1) were observed at 60 s, representing DMPO-OH adducts, which demonstrated the important role of $OH^{\bullet}$. Simultaneously, the characteristic signal of 1:1:1:1:1:1 representing DMPO-SO_4 adducts appeared in the TBC-PMS system, which revealed the

existence of $SO_4^{\bullet -}$. In conclusion, the TBC-PMS system can remove urea mainly through the free radical pathway rather than the non-radical one. Both $OH^{\bullet}$ and $SO_4^{\bullet -}$ were significant in the catalytic process of TBC-PMS system while the contribution of $OH^{\bullet}$ was dominant.

3.4.2 Role of thermally modified biochar

To further explore the generation of free radicals, FTIR and XPS spectra were analyzed, which exhibited the variation of TBC in the reaction. The peak vibration intensity at around 3435 cm^{-1} decreased after the reaction, indicating that –OH might participate the catalytic reaction (see Supplementary Materials). The double peak in the range of 1408- 1472 cm^{-1} and the peak around 864 cm^{-1} vanished. It demonstrated that the carbonates in TBC participated in the catalytic reaction (Jiang et al., 2017; Pan et al., 2021). According to the previous study (Jiang et al., 2017), PMS can be activated to generate HCO_4^- by bicarbonate or carbonate and then HCO_4^- can be further decomposed into other active substances such as $OH^{\bullet}$ and $CO_3^{\bullet -}$. In addition, Zhu et al. (2020) confirmed that CO_3^{2-} can be regarded as an electron donor to accelerate the PMS decomposition. The promoting effect of carbonate was reflected in two ways. One is that carbonate can form HCO_4^- and further decompose into $OH^{\bullet}$ (Eqs. (10) - (11) (Feng et al., 2017; Pan et al., 2021)), resulting in $OH^{\bullet}$ being the main contributor in the catalytic system. The other is that carbonate as an electron donor can facilitate the decomposition of PMS and produce more free radicals ($OH^{\bullet}$ and $SO_4^{\bullet -}$).

$$CO_3^{2-} + HSO_5^- \rightarrow HCO_4^- + SO_4^{2-} \quad (10)$$

$$HCO_4^- \rightarrow CO_3^{\bullet -} + OH^{\bullet} \quad (11)$$

Additionally, the peak vibration intensity near 1059 cm^{-1} was obviously weakened after the reaction. Simultaneously, the peak near 572 cm^{-1} disappeared. This suggested that the phosphate in TBC performed a positive role in the catalytic reaction. It was inferred that the unique asymmetric structure of PMS was the decisive factor for its activation by phosphate anions (PBS) (Lou et al., 2014). Through Density Functional Theory (DFT) calculation, Duan et al. (2021) further confirmed that PBS promoted the degradation of pollutants by accelerating the activation of PMS. Definitively, PO_4^{3-} and HPO_4^{2-} can capture hydroxyl from HSO_5^- and destroy the O-O bond of PMS effectively. This promoted the generation of $SO_4^{\bullet -}$ and decomposition of pollutants. Apart from this, DFT calculation confirmed that the asymmetry of PMS molecules was conducive to its reaction with PBS.

The C1s spectrum of the original TBC could be deconvoluted into three peaks: graphite C/C-C/C-H (284.8 eV), C-O (285.4 eV) and C=O (288.8 eV), respectively (see Supplementary Materials). For used TBC, the C1s spectrum was divided into three peaks corresponding to graphite C/C-C/C-H (284.8 eV), C-O (286.2 eV) and C=O (288.7 eV) (see Supplementary Materials) (Liu et al., 2020). After reaction, the graphite C/C-C/C-H in TBC increased from 55.2% to 60.1% and C=O rose from 6.23% to 6.8%. However, the proportion of C-O was 38.5%, which diminished to 33.1%. Clearly, the C-O content in TBC diminished while the C=O content increased, reflecting the transformation of surface functional groups on TBC. Generally, the shift trend of binding energy can reflect the transfer of electrons (Liu et al., 2014). As can be seen from the O1s spectra of TBC (see Supplementary Materials) after reaction the apparent

left shift of the binding energy for O1s can be observed. It demonstrated that PMS received electrons from O during the reaction. It was caused by the conversion of oxygen functional groups on TBC, which was consistent with the C1s spectra. Based on the above results, it was concluded that some oxygen groups on TBC were conducive to the activation of PMS.

The activation of PMS was related to the transformation of oxygen functional groups. Some studies have confirmed that both radical and non-radical methods can induce the surface oxidation on the catalyst, resulting in the transformation of oxygen functional groups on the catalyst (Duan et al., 2018; Zhou et al., 2020). In this study, C-O as an electron-rich group worked as an active site in TBC-PMS system rather than C=O, which functioned as the electron donor. Active sites can also promote the production of free radicals by activating PMS (Eq. (12) (Ouyang et al., 2019; Yan et al., 2015)).

$$TBC_{surf}\text{-}COH + HSO_5^{2-} \rightarrow TBC_{surf}\text{-}CO^{\bullet} + SO_4^{\bullet -} + H_2O \qquad (12)$$

In view of all the above results, it can be confirmed that the PMS activation through TBC was due to the interaction of inorganic anions (carbonate and phosphate) and oxygen functional group (C-O, -OH). Especially, inorganic anions contributed greatly to the activation of PMS, which was compatible with the results of EC value. After secondary pyrolysis, the inorganic anion and salinity of TBC raised, resulting in a significant increase in EC value, which was conducive to accelerating mass transfer and promoting electron transfer in the reaction process. Thereby, PMS was activated by receiving electrons transferred from the TBC. Interestingly, it was also found that the

specific surface area and pore volume of TBC were less than BC, however the activation effect was much better. It suggested that the impact of specific surface area and pore volume can be ignored in the TBC-PMS system. According to the previous study, the native biochar mainly activated PMS through the interaction of C = C, graphite C, defect structure and oxygen-containing functional groups, and the maximum removal rate could reach 70% (Zhang et al., 2022). After modification, the structure of the pristine biochar may be destroyed and inorganic anions were introduced. Obviously, the removal effect of modified biochar was better, indicating the critical role of inorganic anions in TBC-PMS system.

3.5 Perspectives and recommendations

In this study, the spent coffee ground biochar was simply modified through secondary pyrolysis and then acted as a catalyst to remove urea from reclaimed water. The preparation of modified materials was simple with low cost, which can be an economic and environmental method. In addition, the system of modified biochar activating PMS mainly removed urea through free radicals, which can react strongly with most organics. It can be inferred that this system could be effective for removal of other pollutants which have similar and dissimilar characteristics than that of urea. However, the specific effect needs to be confirmed by further research. In addition, to prove field applicability of this proposed system, it is necessary to verify the TBC-PMS performance for treating real reclaimed water and investigate the reusability of TBC.

4. Conclusion

In this study, BC was modified by secondary pyrolysis and its urea removal effect

via activating PMS system was explored. TBC rarely absorb urea while the TBC-PMS system can degrade urea effectively. Quenching experiments showed that radical pathway was dominant in the catalytic process of TBC-PMS system, especially $OH^{\bullet}$. Specifically, secondary pyrolysis can increase the carbonate and phosphate of TBC, which was decisive in the activation of PMS. As well, C-O and -OH and played a positive role in activating PMS. This system can effectively degrade urea and supply an available process for the UPW production.

E-supplementary data for this work can be found in e-version of this paper online.

Acknowledgements

This research was supported by Tianjin Municipal Science and Technology Bureau of China (Project No. 18PTZWHZ00140, 20JCZDJC00380) and TG Hilyte Environment Technology (Beijing) Co., LTD. (Project No. M-P-0-181001-001).

As Huu Hao Ngo, a corresponding author on this paper, is the Editor of Bioresource Technology, he was blinded to this paper during review, and the paper was independently handled by Samir Kumar Khanal as editor."

References

1. Abdul, L., Si, X., Sun, K. and Si, Y. 2021. Degradation of bisphenol A in aqueous environment using peroxymonosulfate activated with carbonate: Performance, possible pathway, and mechanism. Journal of Environmental Chemical Engineering 9(4), 105419.

2. Choi, J. and Chung, J. 2019. Evaluation of urea removal by persulfate with UV irradiation in an ultrapure water production system. Water Res. 158, 411-416.

3. Choi, J., Kim, J.-O. and Chung, J. 2016. Removal of isopropyl alcohol and methanol in ultrapure water production system using a 185 nm ultraviolet and ion exchange system. Chemosphere 156, 341-346.

4. Clurman, A.M., Rodríguez-Narvaez, O.M., Jayarathne, A., De Silva, G., Ranasinghe, M.I., Goonetilleke, A. and Bandala, E.R. 2020. Influence of surface hydrophobicity/hydrophilicity of biochar on the removal of emerging contaminants. Chem. Eng. J. 402, 126277.

5. Dai, L., Li, L., Zhu, W., Ma, H., Huang, H., Lu, Q., Yang, M. and Ran, Y. 2020. Post-engineering of biochar via thermal air treatment for highly efficient promotion of uranium(VI) adsorption. Bioresour. Technol. 298, 122576.

6. Ding, Y., Fu, L., Peng, X., Lei, M., Wang, C. and Jiang, J. 2022. Copper catalysts for radical and nonradical persulfate based advanced oxidation processes: Certainties and uncertainties. Chem. Eng. J. 427, 131776.

7. Ding, Y., Wang, X., Fu, L., Peng, X., Pan, C., Mao, Q., Wang, C. and Yan, J. 2021. Nonradicals induced degradation of organic pollutants by peroxydisulfate (PDS) and peroxymonosulfate (PMS): Recent advances and perspective. Sci. Total Environ. 765, 142794.

8. Duan, P., Liu, X., Liu, B., Akram, M., Li, Y., Pan, J., Yue, Q., Gao, B. and Xu, X. 2021. Effect of phosphate on peroxymonosulfate activation: Accelerating generation of sulfate radical and underlying mechanism. Applied Catalysis B: Environmental 298,

120532.

9. Duan, X., Sun, H., Shao, Z. and Wang, S. 2018. Nonradical reactions in environmental remediation processes: Uncertainty and challenges. Applied Catalysis B: Environmental 224, 973-982.

10. El-Lateef, H.M.A., Al-Omair, M.A., Touny, A.H. and Saleh, M.M. 2019. Enhanced adsorption and removal of urea from aqueous solutions using eco-friendly iron phosphate nanoparticles. Journal of Environmental Chemical Engineering 7(1), 102939.

11. Feng, Y., Lee, P.-H., Wu, D. and Shih, K. 2017. Surface-bound sulfate radical-dominated degradation of 1,4-dioxane by alumina-supported palladium (Pd/Al2O3) catalyzed peroxymonosulfate. Water Res. 120, 12-21.

12. Gao, Y., Wang, Q., Ji, G. and Li, A. 2022. Degradation of antibiotic pollutants by persulfate activated with various carbon materials. Chem. Eng. J. 429, 132387.

13. Gao, Y., Zhu, Y., Lyu, L., Zeng, Q., Xing, X., Hu, C. 2018. Electronic Structure Modulation of Graphitic Carbon Nitride by Oxygen Doping for Enhanced Catalytic Degradation of Organic Pollutants through Peroxymonosulfate Activation. Environmental Science & Technology, 52(24), 14371-14380.

14. Ghauch, A., Baalbaki, A., Amasha, M., El Asmar, R. and Tantawi, O. 2017. Contribution of persulfate in UV-254nm activated systems for complete degradation of chloramphenicol antibiotic in water. Chem. Eng. J. 317, 1012-1025.

15. Golshan, M., Kakavandi, B., Ahmadi, M. and Azizi, M. 2018. Photocatalytic activation of peroxymonosulfate by TiO2 anchored on cupper ferrite (TiO2@CuFe2O4)

into 2,4-D degradation: Process feasibility, mechanism and pathway. J. Hazard. Mater. 359, 325-337.

16. He, J., Xiao, Y., Tang, J., Chen, H. and Sun, H. 2019. Persulfate activation with sawdust biochar in aqueous solution by enhanced electron donor-transfer effect. Sci. Total Environ. 690, 768-777.

17. Hu, X., Zhang, X., Ngo, H.H., Guo, W., Wen, H., Li, C., Zhang, Y. and Ma, C. 2020. Comparison study on the ammonium adsorption of the biochars derived from different kinds of fruit peel. Sci. Total Environ. 707, 135544.

18. Jiang, M., Lu, J., Ji, Y. and Kong, D. 2017. Bicarbonate-activated persulfate oxidation of acetaminophen. Water Res. 116, 324-331.

19. Kim, D.-G. and Ko, S.-O. 2020. Effects of thermal modification of a biochar on persulfate activation and mechanisms of catalytic degradation of a pharmaceutical. Chem. Eng. J. 399, 125377.

20. Kim, H.-i., Kim, K., Park, S., Kim, W., Kim, S., Kim, J. 2019. Titanium dioxide surface modified with both palladium and fluoride as an efficient photocatalyst for the degradation of urea. Separation and Purification Technology, 209, 580-587.

21. Lee, J., von Gunten, U., Kim, J.-H. 2020a. Persulfate-Based Advanced Oxidation: Critical Assessment of Opportunities and Roadblocks. Environmental Science & Technology, 54(6), 3064-3081.

22. Lee, Y.-C., Li, Y.-f., Chen, M.-J., Chen, Y.-C., Kuo, J. and Lo, S.-L. 2020b. Efficient decomposition of perfluorooctanic acid by persulfate with iron-modified activated carbon. Water Res. 174, 115618.

23. Li, S., Shao, L., Zhang, H., He, P., Lü, F. 2020a. Quantifying the contributions of surface area and redox-active moieties to electron exchange capacities of biochar. Journal of Hazardous Materials, 394, 122541.

24. Li, Z., Sun, Y., Yang, Y., Han, Y., Wang, T., Chen, J., Tsang, D.C.W. 2020b. Biochar-supported nanoscale zero-valent iron as an efficient catalyst for organic degradation in groundwater. Journal of Hazardous Materials, 383, 121240.

25. Liu, H., Liu, Y., Tang, L., Wang, J., Yu, J., Zhang, H., Yu, M., Zou, J. and Xie, Q. 2020. Egg shell biochar-based green catalysts for the removal of organic pollutants by activating persulfate. Sci. Total Environ. 745, 141095.

26. Liu, J., Zou, S., Xiao, L. and Fan, J. 2014. Well-dispersed bimetallic nanoparticles confined in mesoporous metal oxides and their optimized catalytic activity for nitrobenzene hydrogenation. Catalysis Science & Technology 4(2), 441-446.

27. Liu, L., Lin, Y., Liu, Y., Zhu, H. and He, Q. 2013. Removal of Methylene Blue from Aqueous Solutions by Sewage Sludge Based Granular Activated Carbon: Adsorption Equilibrium, Kinetics, and Thermodynamics. J. Chem. Eng. Data 58(8), 2248-2253.

28. Lou, X., Wu, L., Guo, Y., Chen, C., Wang, Z., Xiao, D., Fang, C., Liu, J., Zhao, J. and Lu, S. 2014. Peroxymonosulfate activation by phosphate anion for organics degradation in water. Chemosphere 117, 582-585.

29. Luo, J., Bo, S., Qin, Y., An, Q., Xiao, Z. and Zhai, S. 2020. Transforming goat manure into surface-loaded cobalt/biochar as PMS activator for highly efficient ciprofloxacin degradation. Chem. Eng. J. 395, 125063.

30. Meng, H., Nie, C., Li, W., Duan, X., Bo, L., Ao, Z., Wang, S. and An, T. 2020. Insight into the effect of lignocellulosic biomass source on the performance of biochar as persulfate activator for aqueous organic pollutants remediation: epicarp and mesocarp of citrus peels as examples. J. Hazard. Mater., 123043.

31. Nie, M., Deng, Y., Nie, S., Yan, C., Ding, M., Dong, W., Dai, Y. and Zhang, Y. 2019. Simultaneous removal of bisphenol A and phosphate from water by peroxymonosulfate combined with calcium hydroxide. Chem. Eng. J. 369, 35-45.

32. Ouyang, D., Chen, Y., Yan, J., Qian, L., Han, L. and Chen, M. 2019. Activation mechanism of peroxymonosulfate by biochar for catalytic degradation of 1,4-dioxane: Important role of biochar defect structures. Chem. Eng. J. 370, 614-624.

33. Pan, H., Gao, Y., Li, N., Zhou, Y., Lin, Q. and Jiang, J. 2021. Recent advances in bicarbonate-activated hydrogen peroxide system for water treatment. Chem. Eng. J. 408, 127332.

34. Ren, W., Xiong, L., Yuan, X., Yu, Z., Zhang, H., Duan, X. and Wang, S. 2019. Activation of Peroxydisulfate on Carbon Nanotubes: Electron-Transfer Mechanism. Environ. Sci. Technol. 53(24), 14595-14603.

35. Ridder, M. 2022. Global coffee consumption 2012/13 – 2020/21, ICO@Statista 2022.

36. Tan, C., Fu, D., Gao, N., Qin, Q., Xu, Y. and Xiang, H. 2017. Kinetic degradation of chloramphenicol in water by UV/persulfate system. Journal of Photochemistry and Photobiology A: Chemistry 332, 406-412.

37. Wan, Z., Sun, Y., Tsang, D.C.W., Yu, I.K.M., Fan, J., Clark, J.H., Zhou, Y., Cao,

X., Gao, B., Ok, Y.S. 2019. A sustainable biochar catalyst synergized with copper heteroatoms and CO2 for singlet oxygenation and electron transfer routes. Green Chemistry, 21(17), 4800-4814.

38. Wang, D., Sun, Y., Tsang, D.C.W., Khan, E., Cho, D.-W., Zhou, Y., Qi, F., Gong, J., Wang, L. 2020. Synergistic utilization of inherent halides and alcohols in hydraulic fracturing wastewater for radical-based treatment: A case study of di-(2-ethylhexyl) phthalate removal. Journal of Hazardous Materials, 384, 121321

39. Wang, Q., Lu, X., Cao, Y., Ma, J., Jiang, J., Bai, X. and Hu, T. 2017. Degradation of Bisphenol S by heat activated persulfate: Kinetics study, transformation pathways and influences of co-existing chemicals. Chem. Eng. J. 328, 236-245.

40. Wang, S., Liu, H., Gu, J., Sun, H., Zhang, M. and Liu, Y. 2019. Technology feasibility and economic viability of an innovative integrated ceramic membrane bioreactor and reverse osmosis process for producing ultrapure water from municipal wastewater. Chem. Eng. J. 375, 122078.

41. Wang, S., Meng, Q., Zhu, Q., Niu, Q., Yan, H., Li, K., Li, G., Li, X., Liu, H., Liu, Y. and Li, Q. 2021. Efficient decomposition of lignocellulose and improved composting performances driven by thermally activated persulfate based on metagenomics analysis. Sci. Total Environ. 794, 148530.

42. Wei, X., Gao, N., Li, C., Deng, Y., Zhou, S. and Li, L. 2016. Zero-valent iron (ZVI) activation of persulfate (PS) for oxidation of bentazon in water. Chem. Eng. J. 285, 660-670.

43. Yan, J., Han, L., Gao, W., Xue, S. and Chen, M. 2015. Biochar supported

nanoscale zerovalent iron composite used as persulfate activator for removing trichloroethylene. Bioresour. Technol. 175, 269-274.

44. Yang, J., Zhu, M. and Dionysiou, D.D. 2021. What is the role of light in persulfate-based advanced oxidation for water treatment? Water Res. 189, 116627.

45. Zhang, X., Yang, Y., Hao Ngo, H., Guo, W., Sun, F., Wang, X., Zhang, J. and Long, T. 2022. Urea removal in reclaimed water used for ultrapure water production by spent coffee biochar/granular activated carbon activating peroxymonosulfate and peroxydisulfate. Bioresour. Technol. 343, 126062.

46. Zhang, X., Yang, Y., Ngo, H.H., Guo, W., Wen, H., Wang, X., Zhang, J. and Long, T. 2021. A critical review on challenges and trend of ultrapure water production process. Sci. Total Environ. 785, 147254.

47. Zhong, Q., Lin, Q., He, W., Fu, H., Huang, Z., Wang, Y. and Wu, L. 2021. Study on the nonradical pathways of nitrogen-doped biochar activating persulfate for tetracycline degradation. Sep. Purif. Technol. 276, 119354.

48. Zhou, X., Zeng, Z., Zeng, G., Lai, C., Xiao, R., Liu, S., Huang, D., Qin, L., Liu, X., Li, B., Yi, H., Fu, Y., Li, L. and Wang, Z. 2020. Persulfate activation by swine bone char-derived hierarchical porous carbon: Multiple mechanism system for organic pollutant degradation in aqueous media. Chem. Eng. J. 383, 123091.

49. Zhu, C., Zhang, Y., Fan, Z., Liu, F. and Li, A. 2020. Carbonate-enhanced catalytic activity and stability of Co3O4 nanowires for 1O2-driven bisphenol A degradation via peroxymonosulfate activation: Critical roles of electron and proton acceptors. J. Hazard. Mater. 393, 122395.

50. Zhu, J., Song, Y., Wang, L., Zhang, Z., Gao, J., Tsang, D.C.W., Ok, Y.S. and Hou, D. 2022. Green remediation of benzene contaminated groundwater using persulfate activated by biochar composite loaded with iron sulfide minerals. Chem. Eng. J. 429, 132292.

Figure Captions

Fig. 1. Urea removal effect in the catalytic system (BC concentration: 0.2 g/L, TBC concentration: 0.2 g/L, urea concentration: 1 mg/L; C_0 and C_t represent the urea concentration (mg/L) in the solution before and after the degradation reaction, respectively. (Having the same letter: no significant difference, having different letters: significant difference. Results obtained from ANOVA (α = 0.05))

Fig. 2. The effect of TBC dosage (a), pH (b) and co-existing anions (c) in the TBC/PMS system (PMS concentration: 2 g/L, urea concentration: 1 mg/L; C_0 and C_t represent the urea concentration (mg/L) in the solution before and after the degradation reaction, respectively. (Having the same letter: no significant difference, having different letters: significant difference. Results obtained from ANOVA (α = 0.05))

Fig. 3. (a) Effect of quenching agent on urea removal in TBC-PMS and PMS-only systems (Having the same letter: no significant difference, having different letters: significant difference. Results obtained from ANOVA (α = 0.05)); (b) Contribution of each radical to urea removal.

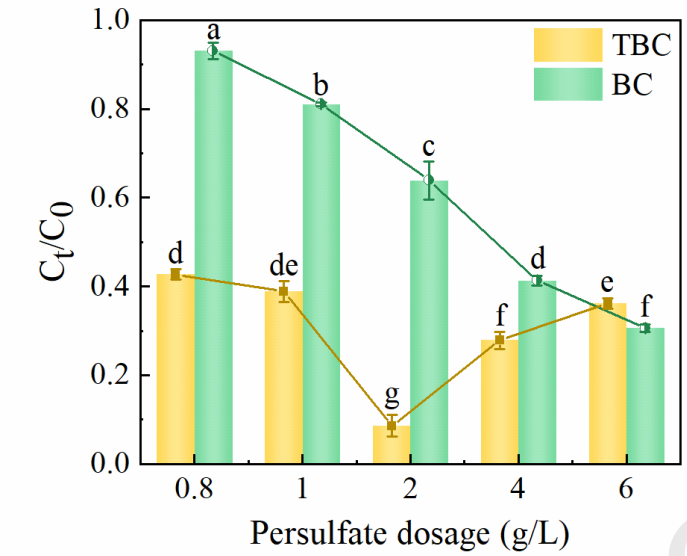

Fig. 1. Urea removal effect in the catalytic system (BC concentration: 0.2 g/L, TBC concentration: 0.2 g/L, urea concentration: 1 mg/L; C_0 and C_t represent the urea concentration (mg/L) in the solution before and after the degradation reaction, respectively. (Having the same letter: no significant difference, having different letters: significant difference. Results obtained from ANOVA (α = 0.05))

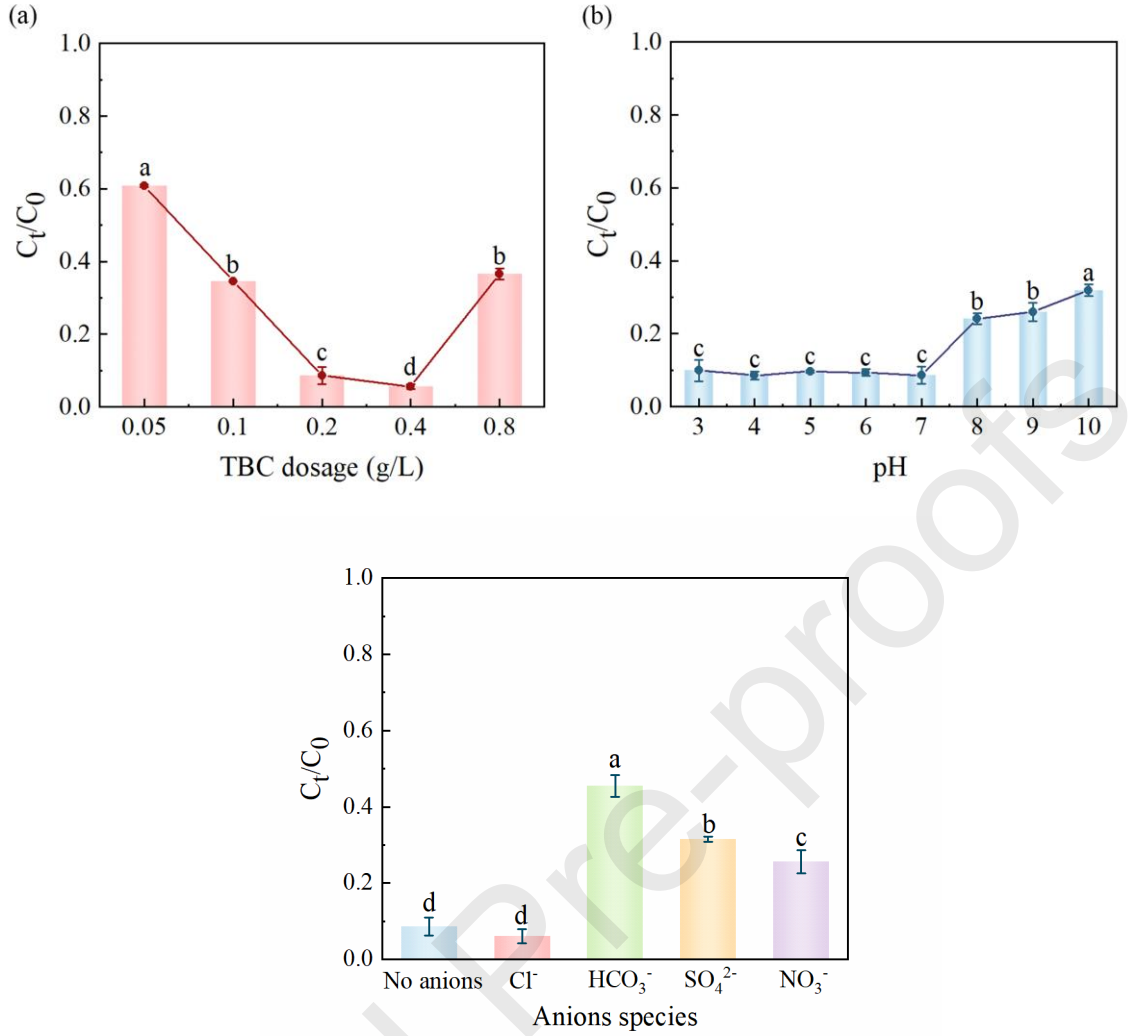

Fig. 2. The effect of TBC dosage (a), pH (b) and co-existing anions (c) in the TBC/PMS system (PMS concentration: 2 g/L, urea concentration: 1 mg/L; C_0 and C_t represent the urea concentration (mg/L) in the solution before and after the degradation reaction, respectively. Having the same letter indicates no significant difference, Different letters indicate significant difference. Results obtained from ANOVA (α = 0.05).)

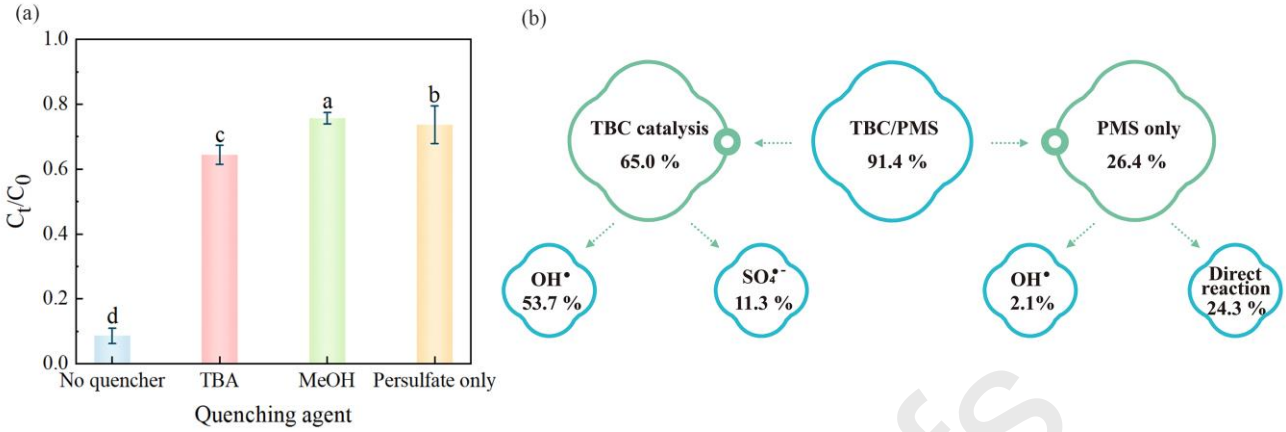

Fig. 3. (a) Effect of quenching agent on urea removal in TBC-PMS and PMS-only systems (Having the same letter indicates no significant difference, Different letters indicate significant difference. Results obtained from ANOVA (α = 0.05).); (b) Contribution of each radical to urea removal.